



THE UNIVERSITY *of* EDINBURGH

Edinburgh Research Explorer

The Origin of Chalcogen-Bonding Interactions

Citation for published version:

Pascoe, D, Ling, K & Cockroft, S 2017, 'The Origin of Chalcogen-Bonding Interactions', *Journal of the American Chemical Society*, vol. 139, no. 42, pp. 15160–15167. <https://doi.org/10.1021/jacs.7b08511>

Digital Object Identifier (DOI):

[10.1021/jacs.7b08511](https://doi.org/10.1021/jacs.7b08511)

Link:

[Link to publication record in Edinburgh Research Explorer](#)

Document Version:

Peer reviewed version

Published In:

Journal of the American Chemical Society

General rights

Copyright for the publications made accessible via the Edinburgh Research Explorer is retained by the author(s) and / or other copyright owners and it is a condition of accessing these publications that users recognise and abide by the legal requirements associated with these rights.

Take down policy

The University of Edinburgh has made every reasonable effort to ensure that Edinburgh Research Explorer content complies with UK legislation. If you believe that the public display of this file breaches copyright please contact openaccess@ed.ac.uk providing details, and we will remove access to the work immediately and investigate your claim.



The Origin of Chalcogen-Bonding Interactions

Dominic J. Pascoe[†], Kenneth B. Ling[‡], and Scott L. Cockroft^{†*}

[†]EaStCHEM School of Chemistry, University of Edinburgh, Joseph Black Building, David Brewster Road, Edinburgh, EH9 3FJ, UK

[‡]Syngenta, Jealott's Hill International Research Centre, Bracknell, Berkshire, RG42 6EY, UK

ABSTRACT: Favorable molecular interactions between group 16 elements have been implicated in catalysis, biological processes, materials and medicinal chemistry. Such interactions have since become known as chalcogen bonds by analogy to hydrogen and halogen bonds. Although the prevalence and applications of chalcogen-bonding interactions continues to develop, debate still surrounds the energetic significance and physicochemical origins of this class of σ -hole interaction. Here, synthetic molecular balances were used to perform a quantitative experimental investigation of chalcogen-bonding interactions. Over 160 experimental conformational free energies were measured in 13 different solvents to examine the energetics of $O\cdots S$, $O\cdots Se$, $S\cdots S$, $O\cdots HC$, and $S\cdots HC$ contacts and the associated substituent and solvent effects. The strongest chalcogen-bonding interactions were found to be at least as strong as conventional H-bonds, but unlike H-bonds, surprisingly independent of the solvent. The independence of the conformational free energies on solvent polarity, polarizability and H-bonding characteristics showed that electrostatic, solvophobic and van der Waals dispersion forces did not account for the observed experimental trends. Instead, a quantitative relationship between the experimental conformational free energies and computed molecular orbital energies was consistent with the chalcogen-bonding interactions being dominated by $n\rightarrow\sigma^*$ orbital delocalization between a lone pair (n) of a (thio)amide donor and the anti-bonding σ^* orbital of an acceptor thiophene or selenophene. Interestingly, stabilization was manifested through the same acceptor molecular orbital irrespective of whether a direct chalcogen \cdots chalcogen, or chalcogen \cdots H-C contact was made. Our results underline the importance of often-overlooked orbital delocalization effects in conformational control and molecular recognition phenomena.

Introduction

It would be reasonable to expect that electron-rich group 16 (chalcogen) elements such as oxygen, sulfur and selenium may not form particularly favorable contacts with each other. However, chalcogen-chalcogen contacts are so commonly observed in X-ray crystal structures that they have become known as chalcogen-bonding interactions.¹⁻³ Chalcogen-bonding interactions have been invoked in such diverse areas as catalytic,^{4,5} synthetic,^{6,7} materials,^{8,9} biological,¹⁰ medicinal,^{1,11} and supramolecular chemistry.¹²⁻¹⁴ Chalcogen-bonding interactions are themselves considered to be a sub-class of “ σ -hole interaction”,¹⁵ which are most well-known for their association with halogen-bonding interactions (group 17).¹⁶⁻¹⁸ Alongside the halogens and chalcogens, tetrel elements (group 14),¹⁹ pnictogens (group 15),^{20,21} and even aerogens (group 18)²² have been identified as being able to engage in σ -hole interactions. Despite the undoubted prevalence of σ -hole interactions, their energetic significance in solution, and the underlying physicochemical origins are the subject of debate.²³⁻³⁰ σ -Holes were originally defined as being associated with a region of positive electrostatic potential that projects along the Z-axis opposite to a σ bond.¹⁵ In line with the original definition, some experimental characteristics of σ -hole interactions can be qualitatively, and sometimes quantitatively, correlated with electrostatic potentials.³⁰⁻³² However, other studies have suggested that dispersion and orbital delocalization effects may also make important contributions.^{17,24,29,33-37} For example, X-ray crystallographic data have revealed the striking directional dependency of some σ -hole interactions, which is consistent with geometry dependent orbital effects.³⁸⁻⁴¹

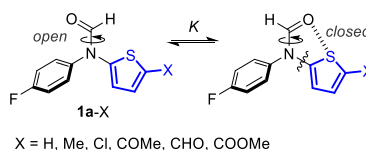
Due to the difficulty associated with the measurement of weak interactions in solution, there remains a paucity of

quantitative experimental investigations of chalcogen-bonding interactions.^{31,36} Furthermore, developing a quantitative understanding of the nature of these interactions is further complicated by the challenges associated with dissecting multiple competing influences and solvent effects, which are both hard to predict, and may dominate the experimental behavior.⁴²⁻⁴⁵

Here we have used synthetic molecular balances (Figure 1) to perform a quantitative experimental investigation of chalcogen-bonding interactions. Experimental conformational free energies were compared with theory to

FORMAMIDE BALANCES

A α -thiophenes



THIOFORMAMIDE BALANCES

D α -thiophenes

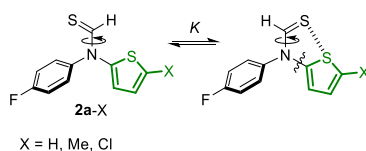


Figure 1. Molecular balances used in the present investigation to investigate chalcogen-bonding interactions.

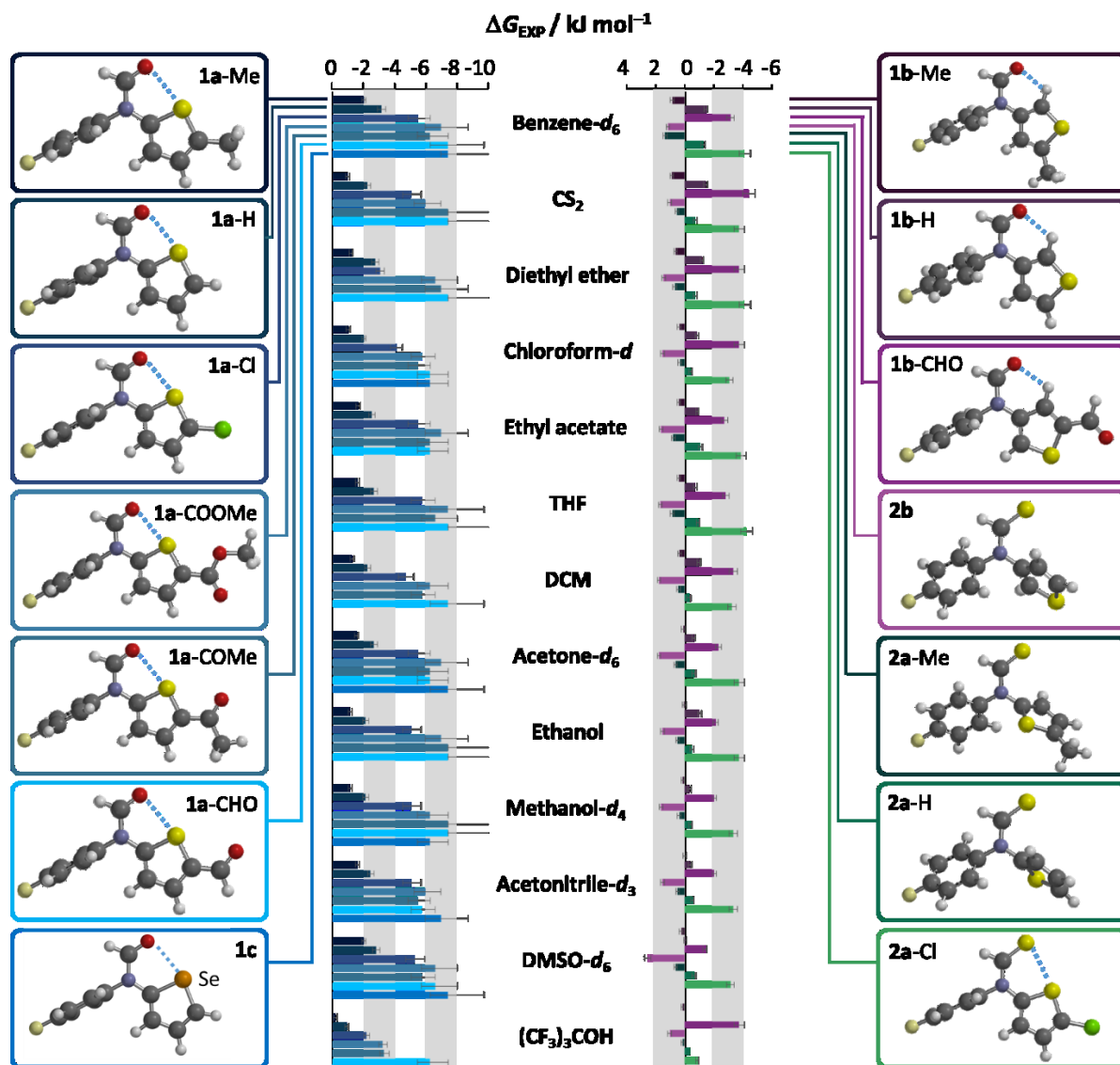


Figure 2. Experimental conformational free energies (ΔG_{EXP}) measured in 13 different solvents at 298 K. Corresponding minimized structures of each of the molecular balances calculated in the gas phase using B3LYP/6-311G* are shown. Colors correspond to those used in structures shown in Figure 1. Where the conformational equilibrium constant, $K > 20$, conformational energies are plotted at -7.4 kJ mol^{-1} with error bars truncated beyond $-10.0 \text{ kJ mol}^{-1}$. All data and errors are tabulated in the SI.

examine the empirical significance of solvent-mediated electrostatic and solvophobic effects (Figure 2), van der Waals dispersion (Figures 2 and 3), and orbital delocalization (Figures 4-7).

Experimental evaluation of chalcogen-bonding interactions

We used molecular balances⁴⁶ for our quantitative experimental investigation of chalcogen-bonding interactions (Figure 1). Molecular balances provide useful tools for the quantification of interactions, since the position of a conformational equilibrium depends on the magnitude of intramolecular interactions and the competing solvent effects (Figure 1A).^{42,43,47,48} Accordingly, molecular balances have been used to measure a wide range of interaction classes including those involving fluorine,⁴⁹⁻⁵¹ arenes,⁵²⁻⁶¹ and carbonyl groups.⁶²⁻⁶⁷ More specifically, the molecular balances shown in Figure 1 are derived from previous investigations of solvent effects and hydrogen bonding interac-

tions.^{42,47,68} The new designs in Figure 1 host chalcogen-bonding interactions in the closed conformers (Figures 1A, D, right) that are absent in the open conformation (Figures 1A, D, left). Since rotation about the (thio)formamide is slow on the NMR timescale at room temperature, integration of the discrete ^{19}F NMR resonances corresponding to each conformer provides direct access to the conformational equilibrium constant, K and therefore the conformational free energy difference, $\Delta G_{\text{EXP}} = -RT \ln K$.

The compounds shown in Figure 1 containing a range of potential O, S and Se contacts were synthesized (see SI). An X-ray crystal structure of balance **1a-Cl** (CSD deposition no. 1563020) and density functional theory (DFT) calculations confirmed that most of the α -substituted **1a** and **2a** series of molecular balances accommodated chalcogen \cdots chalcogen contacts in the closed conformation (Figures 2, S10-S12). In addition, balances containing β -substituted thiophenes that were incapable of forming direct chalcogen \cdots chalcogen contacts in the closed

conformer were synthesized with the intention of serving as controls (**1b** series and **2b**, Figure 1B, E). Conformers were assigned using HMBC / NOESY NMR spectroscopy and by the comparison of experimental and computed conformational ratios (see SI and below). The conformational free energy differences between the open and closed conformers were measured for each balance in 13 different solvents (Figure 2).

All of the compounds in series **1a** and **1c** preferred the closed conformers in which O \cdots S, or O \cdots Se contacts were formed (<-7.4 to -1 kJ mol $^{-1}$). Such conformational preferences are comparable to those of OH to O=C H-bonds measured in structurally related molecular balances.⁶⁸ Varying the thiophene substituent had a substantial influence on the preference for O \cdots S contacts, following the trend Me < H < Cl < COOMe < COMe < COH (Figure 2, left). Interestingly, the O \cdots Se contact in compound **1c** was slightly more favorable than the O \cdots S contact in compound **1a**-COH, despite the increased steric bulk and the lack of an electron-withdrawing group on the selenophene ring. β -Thiophene compounds **1b**-H and **1b**-COH, which could not form O \cdots S contacts had a weaker preference for the closed conformer compared to the corresponding α -thiophenes **1a**-H and **1a**-COH that could form direct O \cdots S contacts. Thioformamide balances **2a**-Me, **2a**-H, **2a**-Cl that could potentially host S \cdots S contacts had ~ 1.5 kJ mol $^{-1}$ decreased preference for the closed conformer compared to the equivalently substituted **1a** balances that hosted O \cdots S contacts. Indeed, while balances in series **1a** and **1c** had minimized structures containing planar O \cdots S or O \cdots Se contacts, such a planar structure and corresponding S \cdots S contact was only seen in balance **2a**-Cl. Similarly, β -thiophenes in the **1b** series were calculated to have planar structures, hosting C=O \cdots HC contacts, while the equivalent β -substituted thioformamide **2b** did not, and instead adopted a propeller-like conformation. Consistent with previous studies,¹ there was little difference in the energies of secondary conformers in which X/Y-carbonyl substituents were flipped, suggesting that no significant secondary chalcogen \cdots chalcogen interactions were present in the X/Y-carbonyl substituted compounds.⁶⁹

Evaluation of solvent-mediated electrostatic and solvophobic contributions

Solvents are known to exert both electrostatic (including H-bonding interactions) and solvophobic influences on the conformational preferences of molecular balances.^{42-45,47,48,60,70} The conformational free energy differences in Figure 2 show striking solvent independence for balances that preferred the closed conformation. For example, conformational free energies across compound series **1** were similar in solvophobic H-bonding solvents such as methanol-*d*₄ and dimethylsulfoxide-*d*₆ compared to very apolar solvents, such as carbon disulfide and benzene-*d*₆. The only significant solvent-dependent changes in conformational free energies were seen when the very strong H-bond donor perfluoro-*tert*-butanol was used as a solvent. Conformational free energies in this solvent were found to be driven towards the open conformer by ~ 2 kJ mol $^{-1}$ compared to the other solvents due to its ability to form strong competitive H-bonding interactions with formyl carbonyl groups (Figure 2, bottom). There have been previous reports of very weak solvent effects on some other σ -hole interactions,^{29,33,34,71,72} but such observations are not universal.³¹ The lack of solvent dependence in the present investigation is particularly surprising considering that the conformational free energies of similar formamide

molecular balances hosting H-bonding and aromatic interactions were found to be strongly dependent on the H-bond donor and acceptor abilities of the solvent.^{42,68} These findings indicate that the chalcogen-bonding interactions in the present investigation do not have a substantial solvophobic, electrostatic or dipolar origin (Table S18). Although, the balances in the present investigation were not soluble in water, given the apparent universality of the observed independence, it might be reasonable to expect similar conformational preferences in aqueous solution.

Evaluation of van der Waals dispersion contributions

Having ruled out substantial solvophobic and electrostatic contributions to chalcogen-bonding interactions in our investigation, we then set out to consider van der Waals dispersion forces. Bulk solvent polarizability has been shown to describe the extent to which the solvent competes with, and attenuates dispersion forces between functional groups.^{43,73} Solvents with low bulk polarizability would be expected to favor closed conformers that accommodate chalcogen \cdots chalcogen interactions involving polarizable S and Se atoms, while highly polarizable solvents would be expected to favor the open conformer to expose polarizable groups to the solvent. However, Figure 2 shows that there is a negligible difference between the conformational free energies measured in the highly polarizable solvent carbon disulfide, compared to methanol-*d*₄, which has a low bulk polarizability.⁴³ The solvent with the lowest bulk polarizability in our investigation is perfluoro-*tert*-butanol, which should favor the closed conformer if contributions from dispersion forces in the chalcogen \cdots chalcogen contacts are significant. Instead, the conformational free energies in perfluoro-*tert*-butanol are driven towards the open conformer compared to all of the other solvents. This indicates that solvation of the formyl oxygen atoms by hydrogen bonding is more energetically significant than any contribution from residual differences in dispersion forces in the solution phase. Furthermore, the experimental conformational free energies were compared with those calculated in the gas-phase using DFT methods that both did, and did not, include dispersion corrections (M06-2X and ω B97X-D vs. B3LYP). The strongest correlation was found against conformational energies (ΔE_{CALC}) calculated using the non-dispersion corrected B3LYP method ($R^2 = 0.94$, Figure 3A). In contrast, conformational energies calculated using dispersion-corrected (DFT-D) methods formed substantially poorer correlations ($R^2 = 0.88$ and 0.84 , Figures 3B-C). Thus, these correlations, combined with the very limited solvent dependence of the conformational free energies indicate that differences in dispersion forces make negligible contributions to the chalcogen-bonding interactions that govern the observed conformational free energies.

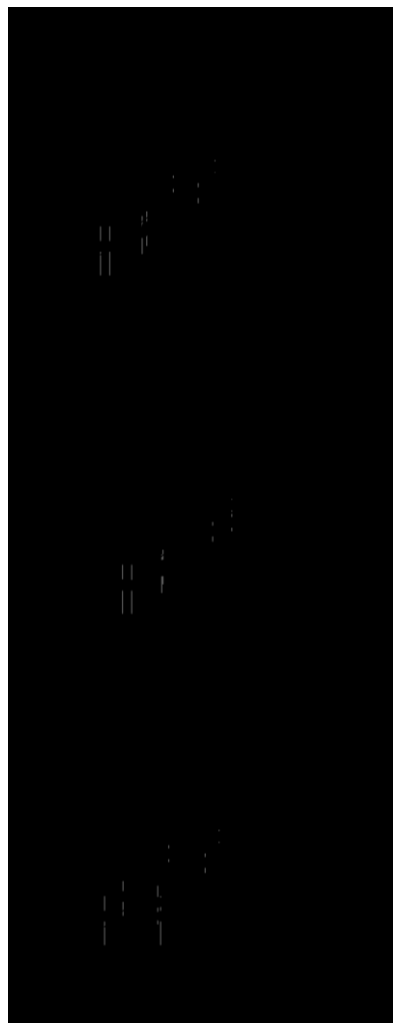


Figure 3. Correlations of experimental conformational free energies measured in CDCl_3 at 298 K (ΔG_{EXP}) vs. those predicted at the indicated levels of theory in the gas phase (ΔE_{CALC}). An additional correlation using the SM8 implicit solvent model for chloroform showed no improvement in the correlation coefficient (Figure S23).

Evaluation of orbital delocalization contributions

So far, we have discounted electrostatic, solvophobic and dispersion forces as the primary determinants of the chalcogen-bonding interactions in our molecular balances. Others have proposed that orbital delocalization effects may play a role in various classes of σ -hole interactions based on spectroscopic, structural and computational analyses.^{17,24,29,33-41} Delocalization effects are long recognized aspects of bond theory; most chemists are familiar with the concepts of inductive polarization along σ -bonds, resonance involving π -bonds, and hyperconjugation between σ - and π -bonds. However, similar forms of orbital delocalization are commonly overlooked in the context of molecular interactions, which are often considered to be “non-bonding”, or “non-covalent”. We point out that the terminology used to describe electron delocalization effects in “non-bonded” interactions is often inconsistent: polarization, donor-acceptor interactions, charge transfer, partial covalency, orbital mixing, and orbital interactions, among others, have all been used to describe a broadly similar ground-state phenomenon.^{11,32,74-78} Such inconsistencies may arise, at least in part, from the chal-

lenge of obtaining systematic, direct experimental measurements of weak interactions in solution, and further establishing causal association with quantum mechanical descriptors.⁷⁷

Nonetheless, $n \rightarrow \pi^*$ orbital delocalization from a lone pair (n) into the carbonyl antibonding orbital (π^*) has been proposed to stabilize carbonyl-carbonyl interactions,⁶²⁻⁶⁶ alongside competing dipolar electrostatic explanations.⁶⁷ Similarly, $n \rightarrow \sigma^*$ delocalization from a lone pair orbital (n) into the antibonding orbital of a σ -bond (σ^*) has been suggested by theory to stabilize interactions involving chalcogens.^{24,29,33-41,79} Thus, we set about performing a comprehensive orbital analysis of our molecular balances.

Our orbital analysis began by performing geometry minimizations on the open and closed conformations of molecular balances bearing a range of substituents (all of the compounds shown in Figure 1 and more, see SI) using both DFT and DFT-D methods. We hypothesized that the energies of particular orbitals in the open and closed conformers could be compared to reveal orbital interactions that specifically stabilized one conformer over the other. To avoid the splitting of the orbitals arising from the canonical resonance forms of the aromatic electrons that were not involved in the chalcogen interactions, the fluorophenyl moiety was replaced with a proton, and a single-point energy calculation performed on each structure (retaining the geometry of the complete balance). The use of such fragments greatly simplified the task of assigning pairs of open/closed orbitals (see SI for validation). The resulting comparison of orbital energies for all of the balances with planar structures from Figure 2 is presented in Figure 4. The line formed by the gray points in Figure 4A corresponds to the vast

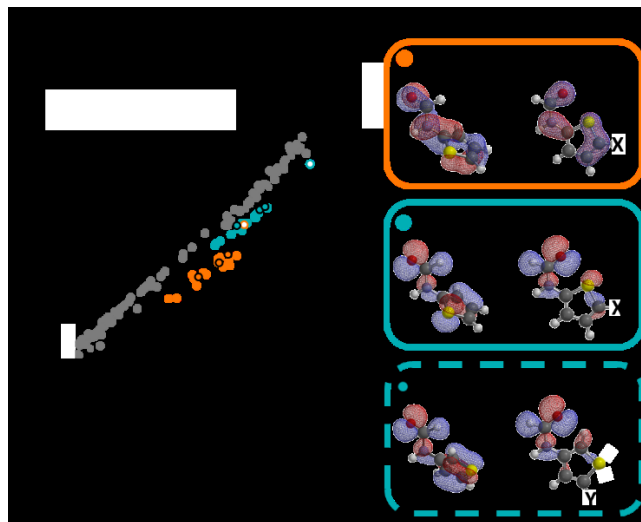


Figure 4. (A) Correlation of calculated orbital energies in the open vs. closed molecular balance conformers. Data points that fall below the line formed by the gray points are stabilized in the closed conformer due to (B) resonance delocalization modulated by structural planarization (orange), and $n \rightarrow \sigma^*$ orbital delocalization (teal) arising from either (C) direct chalcogen...chalcogen contacts, or (D) chalcogen...H-C contacts. Solid filled points are orbital energies for α -thiophene series **1a-X** and α -selenophene balance **1c**. Points with black outlines are the β -thiophene balances in the **1b-Y** series. Unfilled circles correspond to the only thioformamide balance hosting a favorable S-S contact, **2a-Cl**. Alternative correlations using M06-2X/6-311G* and ω B97X-D/6-311G*, plus a comparison of full vs. simplified molecular balance data are provided in the SI.

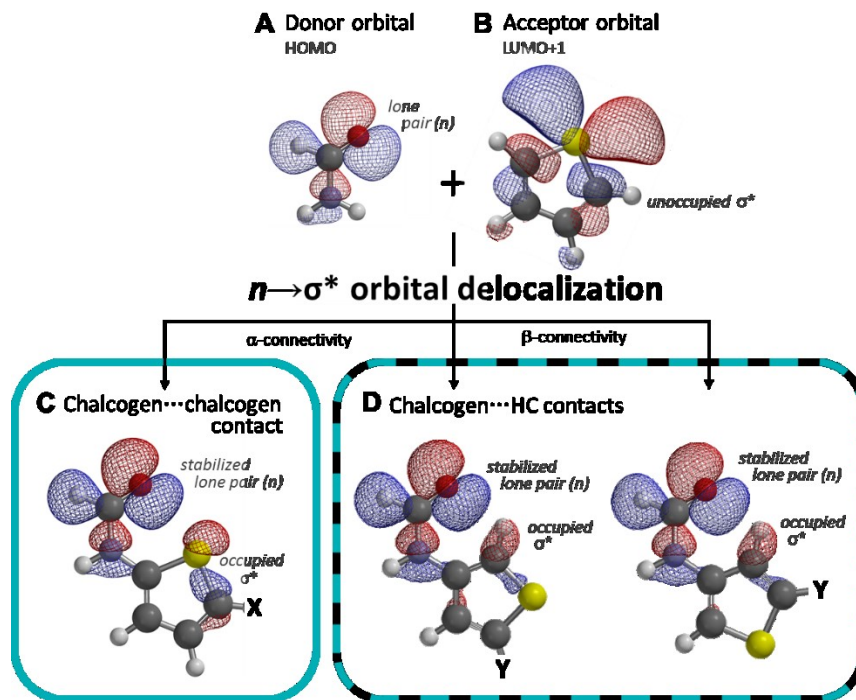


Figure 5. Orbital decomposition analysis illustrating the hypothetical combination of molecular fragments A + B in the three orientations shown. (A) The HOMO containing the formyl oxygen lone pair (n) is stabilized in (C) and (D) by the same set of antibonding σ^* orbitals of the (seleno/thio)phene fragment, irrespective of the orientation of the connected ring and the specific intramolecular contacts present. The preferred conformers of the compounds investigated are shown in Figure 2. All orbitals and minimized geometries were calculated using B3LYP/6-311G*.

majority of orbitals in which there is little difference in energy between the open and closed conformers. Data points that fall below the gray background line correspond to orbitals that are more stable in the closed than the open conformer. Two sets of data sit below the background line (orange and teal, Figure 4A). Upon inspection of the molecular orbitals, the orange data were found to correspond to through-bond, resonance delocalization of the lone pair orbital that lies above and below the plane of the amide into the co-planar aromatic system (orange, Figure 4B). Such delocalized orbitals were accordingly, only present in molecular balances that had planar closed conformations. The teal series corresponded to orbitals in which the other, orthogonal lone pair orbital of the amide was delocalized into the S-C (or Se-C) σ -bond of the adjacent thiophene (or selenophene) (Figures 4C-D and 5C-D). Thus, these orbitals were consistent with the occurrence of stabilizing $n \rightarrow \sigma^*$ orbital interactions.

We confirmed the identity of these delocalized $n \rightarrow \sigma^*$ orbitals by further decomposition of the molecular balance fragments into the constituent (thio)formamide (e.g. Figure 5A) and thiophene (or selenophene) components (e.g. Figure 5B). This hypothetical decomposition analysis indicated that the stabilized, delocalized orbitals of the type shown in Figures 4C-D and 5C-D did indeed result from the hybridization of a high-energy, but occupied, lone pair orbital (Figure 5A) with an even higher energy, unoccupied, anti-bonding molecular orbital of the thiophene (or selenophene) (Figure 5B). Interestingly, this decomposition analysis showed that the same molecular orbitals (Figures 5A-B) combine to stabilize the formamide lone

pair, irrespective of the α/β -connectivity, or the orientation of the thiophene ring (Figure 5C-D). Furthermore, we used Natural Bond Orbital (NBO)⁷⁶ analysis to examine the occurrence and stabilizing character of specific $n \rightarrow \sigma^*$ orbital interactions. In simplistic terms, NBOs are theoretical constructs that are intermediate between molecular orbitals (such as those shown in Figure 5) and the constituent atomic orbitals.⁸⁰ NBOs reveal orbital delocalization that includes both covalent bonds and orbital interactions that can be considered as having “partial” covalent character. Indeed, NBO analysis has previously been used to analyze putative $n \rightarrow \sigma^*$ and $n \rightarrow \pi^*$ interactions.^{29,33-36,65,66} NBO analysis of our balances revealed the potential for stabilizing $n \rightarrow \sigma_{S-C}^*$ and $n \rightarrow \sigma_{Se-C}^*$ delocalization where direct chalcogen...chalcogen contacts occurred, while weaker $n \rightarrow \sigma_{C-S}^*$, $n \rightarrow \sigma_{H-C}^*$, and $n \rightarrow \sigma_{C-C}^*$ NBOs were present in the β -connected thiophene balances (Figure S23 and Table S45).

The occurrence of such orbital interactions should be indicated by lengthening of the accepting bond in the closed conformer relative to the open conformer of each molecular balance. Computational geometry minimizations revealed lengthening of the bonds aligned with the (thio)amide contact in the closed conformation (blue bonds, Figure 6). The extent of bond lengthening did not correlate with the experimental conformational free energies measured in the molecular balances, since changes in electron density were also modulated by the adjacent X and Y substituents (Figure 1). Consistent with this suggestion, bond lengthening also occurred at electron-accepting substituents (purple bonds, Figure 6).

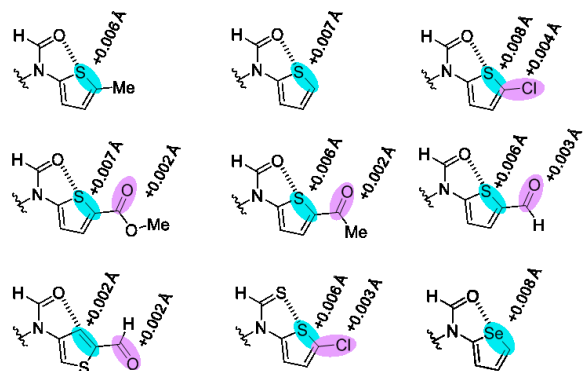


Figure 6. Calculated bond lengthening (B3LYP/6-311G*) in the closed vs. open conformers for molecular balances hosting chalcogen-chalcogen contacts. Further bond length differences are provided in Figure S13.

Having confirmed the identity and possible stabilizing nature of $n \rightarrow \sigma^*$ orbital contributions to chalcogen-bonding interactions, we sought a quantitative energetic relationship between experiment and theory. Unfortunately, we found no correlation between the experimental conformational free energy differences measured in the molecular balances and the $n \rightarrow \sigma^*$ orbital delocalization energies output from the NBO calculations (Figure S22 and Table S45). Indeed, one limitation of NBO analysis is that it can be challenging to ascribe an easily understood physical meaning to NBOs. Instead, we compared the computed energies of physically relevant molecular orbitals with our experimental conformational free energies. A striking correlation was found between the energies of the molecular orbitals identified in Figure 5C-D that contained $n \rightarrow \sigma^*$ orbital delocalization ($R^2 = 0.99$, Figure 7A). The energies relating to balances containing both direct chalcogen \cdots chalcogen and chalcogen \cdots H-C contacts (teal and black outlined points, respectively) were found to fit on the same correlation. This finding was consistent with the involvement of the same σ^* acceptor orbital (Figure 5C-D), irrespective of the orientation or connectivity of the thiophene ring. Contrasting with previous suggestions,⁷⁹ the β -connected thiophenes (black outlines in Figure 7A) were weaker lone pair acceptors than the equivalently substituted α -connected variants (filled circles in Figure 7A). However, it is important to note that the relative acceptor abilities may not be general, as they are likely to be influenced by the geometric constraints imposed by our intramolecular system. The single point associated with selenophene balance **1c** was an outlier (Figure S19) indicating the increased favorability of this interaction compared to the O \cdots S and S \cdots S interactions. In comparison, the energies of the resonance delocalized orbitals (Figure 7B), along with other molecular orbitals (Figure S21) did not form good correlations with the same experimental data. Thus, the strong correlation in Figure 7A establishes a quantitative link between the experimentally determined conformational free energies and the theoretically determined energies of $n \rightarrow \sigma^*$ delocalized orbitals involved in stabilizing the chalcogen-bonding interactions.

Conclusion

We have performed a quantitative, experimental investigation of chalcogen-bonding interactions. Synthetic molecular balances were used to examine solvent and substituent effects on a range of chalcogen \cdots chalcogen and chalcogen \cdots HC contacts

(Figure 1). The conformational free energies of balances hosting chalcogen-bonding interactions were found to be surprisingly solvent independent, ruling out substantial contributions from electrostatic and solvophobic effects (Figure 2).⁸¹ This solvent independence combined with comparison against

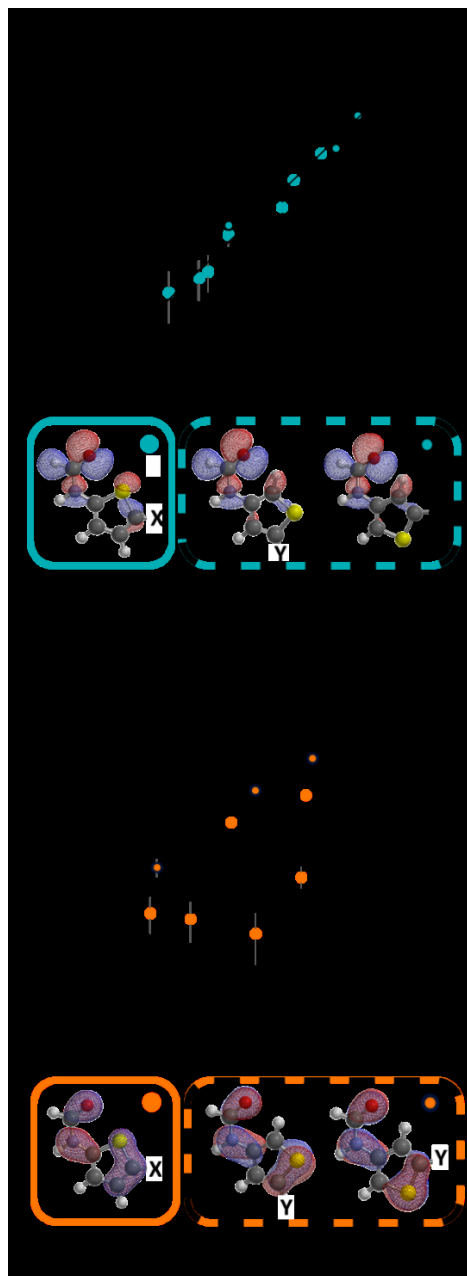


Figure 7. Correlations of the calculated energies of orbitals stabilized by (A) $n \rightarrow \sigma^*$ orbital delocalization (teal), and (B) resonance delocalization modulated by planarization (orange). Solid filled points correspond to α -substituted thiophenes, while β -substituted thiophenes are indicated with black outlines. Calculations were performed on structures of the type shown inset using B3LYP/6-311G*. X and Y = the substituents as shown in Figure 1. Alternative correlations using DFT-D methods are provided in the SI.

dispersion-corrected calculated conformational energies further indicated that van der Waals dispersion forces did not account for the observed interaction trends (Figure 3). The latter finding

was consistent with previous studies that have found substantial attenuation of dispersion forces between functional groups due to competitive dispersion interactions with the surrounding solvent.^{43,61,70,73} Instead, computed changes in bond lengths and NBO analysis pointed towards the involvement of stabilizing contributions from $n \rightarrow \sigma^*$ orbital delocalization between the lone pair on a (thio)amide donor and the antibonding σ^* orbitals of the adjacent thiophene (or selenophene) acceptor. A quantitative relationship between the energy of the orbital hosting $n \rightarrow \sigma^*$ orbital delocalization and the experimental data was seen. Interestingly, thiophene rings were found to accept electrons into the same antibonding molecular orbital in both α - and β -connected thiophenes, either via direct chalcogen...chalcogen or chalcogen...HC contacts. Intriguingly, our quantitative comparison of experimental and computational data reveals empirical behavior most consistent with a dominant contribution from orbital delocalization.^{29,33-36} Our results highlight the energetic significance of orbital delocalization in molecular interactions.

ASSOCIATED CONTENT

Supporting Information. Experimental, characterization and computational data. Crystallographic data for compound **1a-Cl** was deposited in the CSD with deposition number 1563020.

AUTHOR INFORMATION

Corresponding Author

*scott.cockroft@ed.ac.uk

Author Contributions

The manuscript was written through contributions of all authors.

Funding Sources

We thank Syngenta and the EPSRC for funding.

Acknowledgements

We thank Dr Stefan Borsley for helpful feedback.

ABBREVIATIONS

NMR, nuclear magnetic resonance. DMSO, dimethylsulfoxide. THF, tetrahydrofuran. DCM, dichloromethane.

REFERENCES⁸²

- Beno, B. R.; Yeung, K.-S.; Bartberger, M. D.; Pennington, L. D.; Meanwell, N. A., *J. Med. Chem.* **2015**, *58*, 4383-4438.
- Murray, J. S.; Lane, P.; Politzer, P., *Int. J. Quantum Chem* **2008**, *108*, 2770-2781.
- Murray, J. S.; Lane, P.; Clark, T.; Politzer, P., *J. Mol. Model.* **2007**, *13*, 1033-1038.
- Benz, S.; López-Andarias, J.; Mareda, J.; Sakai, N.; Matile, S., *Angew. Chem. Int. Ed.* **2017**, *56*, 812-815.
- Robinson, E. R. T.; Walden, D. M.; Fallan, C.; Greenhalgh, M. D.; Cheong, P. H.-Y.; Smith, A. D., *Chem. Sci.* **2016**, *7*, 6919-6927.
- Shiina, I.; Nakata, K.; Ono, K.; Onda, Y.-s.; Itagaki, M., *J. Am. Chem. Soc.* **2010**, *132*, 11629-11641.
- Cox, P. A.; Leach, A. G.; Campbell, A. D.; Lloyd-Jones, G. C., *J. Am. Chem. Soc.* **2016**, *138*, 9145-9157.
- Mahmudov, K. T.; Kopylovich, M. N.; Guedes da Silva, M. F. C.; Pombeiro, A. J. L., *Dalton Trans.* **2017**, *46*, 10121-10138.
- Werz, D. B.; Gleiter, R.; Rominger, F., *J. Am. Chem. Soc.* **2002**, *124*, 10638-10639.
- Fick, R. J.; Kroner, G. M.; Nepal, B.; Magnani, R.; Horowitz, S.; Houtz, R. L.; Scheiner, S.; Trievel, R. C., *ACS Chem. Biol.* **2016**, *11*, 748-754.
- Reid, R. C.; Yau, M.-K.; Singh, R.; Lim, J.; Fairlie, D. P., *J. Am. Chem. Soc.* **2014**, *136*, 11914-11917.
- Lim, J. Y. C.; Marques, I.; Thompson, A. L.; Christensen, K. E.; Félix, V.; Beer, P. D., *J. Am. Chem. Soc.* **2017**, *139*, 3122-3133.
- Gleiter, R.; Werz, D. B.; Rausch, B. J., *Chem. Eur. J.* **2003**, *9*, 2676-2683.
- Robinson, S. W.; Mustoe, C. L.; White, N. G.; Brown, A.; Thompson, A. L.; Kennepohl, P.; Beer, P. D., *J. Am. Chem. Soc.* **2015**, *137*, 499-507.
- Murray, J. S.; Lane, P.; Politzer, P., *J. Mol. Model.* **2008**, *15*, 723-729.
- Beale, T. M.; Chudzinski, M. G.; Sarwar, M. G.; Taylor, M. S., *Chem. Soc. Rev.* **2013**, *42*, 1667-1680.
- Cavallo, G.; Metrangolo, P.; Milani, R.; Pilati, T.; Priimagi, A.; Resnati, G.; Terraneo, G., *Chem. Rev.* **2016**, *116*, 2478-2601.
- Clark, T.; Hennemann, M.; Murray, J. S.; Politzer, P., *J. Mol. Model.* **2006**, *13*, 291-296.
- Bauzá, A.; Mooibroek, T. J.; Frontera, A., *Angew. Chem. Int. Ed.* **2013**, *52*, 12317-12321.
- Murray, J. S.; Lane, P.; Politzer, P., *Int. J. Quantum Chem* **2007**, *107*, 2286-2292.
- Zahn, S.; Frank, R.; Hey-Hawkins, E.; Kirchner, B., *Chem. Eur. J.* **2011**, *17*, 6034-6038.
- Bauzá, A.; Frontera, A., *Angew. Chem. Int. Ed.* **2015**, *54*, 7340-7343.
- Burling, F. T.; Goldstein, B. M., *J. Am. Chem. Soc.* **1992**, *114*, 2313-2320.
- Bleiholder, C.; Gleiter, R.; Werz, D. B.; Köppel, H., *Inorg. Chem.* **2007**, *46*, 2249-2260.
- Cozzolino, A. F.; Vargas-Baca, I.; Mansour, S.; Mahmoudkhani, A. H., *J. Am. Chem. Soc.* **2005**, *127*, 3184-3190.
- Esraili, M. D.; Mohammadian-Sabet, F., *Chem. Phys. Lett.* **2015**, *634*, 210-215.
- Murray, J. S.; Lane, P.; Clark, T.; Riley, K. E.; Politzer, P., *J. Mol. Model.* **2012**, *18*, 541-548.
- Duarte, D. J. R.; Sosa, G. L.; Peruchena, N. M., *J. Mol. Model.* **2013**, *19*, 2035-2041.
- Iwaoka, M.; Komatsu, H.; Katsuda, T.; Tomoda, S., *J. Am. Chem. Soc.* **2004**, *126*, 5309-5317.
- Stone, A. J., *J. Am. Chem. Soc.* **2013**, *135*, 7005-7009.
- Garrett, G. E.; Gibson, G. L.; Straus, R. N.; Seferos, D. S.; Taylor, M. S., *J. Am. Chem. Soc.* **2015**, *137*, 4126-4133.
- Politzer, P.; Murray, J. S.; Clark, T., *Phys. Chem. Chem. Phys.* **2013**, *15*, 11178-11189.
- Iwaoka, M.; Komatsu, H.; Katsuda, T.; Tomoda, S., *J. Am. Chem. Soc.* **2002**, *124*, 1902-1909.
- Barton, D. H. R.; Hall, M. B.; Lin, Z.; Parekh, S. I.; Reibenspies, J., *J. Am. Chem. Soc.* **1993**, *115*, 5056-5059.
- Komatsu, H.; Iwaoka, M.; Tomoda, S., *Chem. Commun.* **1999**, 205-206.
- Iwaoka, M.; Tomoda, S., *J. Am. Chem. Soc.* **1996**, *118*, 8077-8084.
- Bleiholder, C.; Werz, D. B.; Köppel, H.; Gleiter, R., *J. Am. Chem. Soc.* **2006**, *128*, 2666-2674.
- Bauza, A.; Quinonero, D.; Deya, P. M.; Frontera, A., *CrystEngComm* **2013**, *15*, 3137-3144.
- Iwaoka, M.; Takemoto, S.; Tomoda, S., *J. Am. Chem. Soc.* **2002**, *124*, 10613-10620.
- Rittner, R.; Ducati, L. C.; Tormena, C. F.; Fiorin, B. C.; Braga, C. B., *Spectrochim. Acta A: Mol. Biomol. Spect.* **2011**, *79*, 1071-1076.
- Hudson, B.; Nguyen, E.; Tantillo, D. J., *Org. Biomol. Chem.* **2016**, *14*, 3975-3980.
- Mati, I. K.; Adam, C.; Cockroft, S. L., *Chem. Sci.* **2013**, *4*, 3965-3965.
- Adam, C.; Yang, L.; Cockroft, S. L., *Angew. Chem. Int. Ed.* **2015**, *54*, 1164-1167.

- (44) Cockroft, S. L.; Hunter, C. A., *Chem. Commun.* **2009**, 3961-3963.
- (45) Cockroft, S. L.; Hunter, C. A., *Chem. Commun.* **2006**, 3806-3808.
- (46) Mati, I. K.; Cockroft, S. L., *Chem. Soc. Rev.* **2010**, *39*, 4195-4205.
- (47) Muchowska, K. B.; Adam, C.; Mati, I. K.; Cockroft, S. L., *J. Am. Chem. Soc.* **2013**, *135*, 9976-9979.
- (48) Yang, L.; Adam, C.; Cockroft, S. L., *J. Am. Chem. Soc.* **2015**, *137*, 10084-10087.
- (49) Hof, F.; Scofield, D. M.; Schweizer, W. B.; Diederich, F., *Angew. Chem., Int. Ed. Eng.* **2004**, *43*, 5056-5059.
- (50) Li, P.; Maier, J. M.; Vik, E. C.; Yehl, C. J.; Dial, B. E.; Rickher, A. E.; Smith, M. D.; Pellechia, P. J.; Shimizu, K. D., *Angew. Chem. Int. Ed.* **2017**, *56*, 7209-7212.
- (51) Ams, M. R.; Fields, M.; Grabnic, T.; Janesko, B. G.; Zeller, M.; Sheridan, R.; Shay, A., *J. Org. Chem.* **2015**, *80*, 7764-7769.
- (52) Maier, J. M.; Li, P.; Hwang, J.; Smith, M. D.; Shimizu, K. D., *J. Am. Chem. Soc.* **2015**, *137*, 8014-8017.
- (53) Tatko, C. D.; Waters, M. L., *J. Am. Chem. Soc.* **2002**, *124*, 9372-9373.
- (54) Gung, B. W.; Wekesa, F.; Barnes, C. L., *J. Org. Chem.* **2008**, *73*, 1803-1808.
- (55) Newcomb, L. F.; Gellman, S. H., *J. Am. Chem. Soc.* **1994**, *116*, 4993-4994.
- (56) Kim, E.-i.; Paliwal, S.; Wilcox, C. S., *J. Am. Chem. Soc.* **1998**, *120*, 11192-11193.
- (57) Paliwal, S.; Geib, S.; Wilcox, C. S., *J. Am. Chem. Soc.* **1994**, *116*, 4497-4498.
- (58) Gardarsson, H.; Schweizer, W. B.; Trapp, N.; Diederich, F., *Chem. Eur. J.* **2014**, *20*, 4608-4616.
- (59) Motherwell, W. B.; Moise, J.; Aliev, A. E.; Nič, M.; Coles, S. J.; Horton, P. N.; Hursthouse, M. B.; Chessari, G.; Hunter, C. A.; Vinter, J. G., *Angew. Chem. Int. Ed.* **2007**, *46*, 7823-7826.
- (60) Emenike, B. U.; Bey, S. N.; Bigelow, B. C.; Chakravartula, S. V. S., *Chem. Sci.* **2016**, *7*, 1401-1407.
- (61) Hwang, J.; Dial, B. E.; Li, P.; Kozik, M. E.; Smith, M. D.; Shimizu, K. D., *Chem. Sci.* **2015**, *6*, 4358-4364.
- (62) Bartlett, G. J.; Newberry, R. W.; VanVeller, B.; Raines, R. T.; Woolfson, D. N., *J. Am. Chem. Soc.* **2013**, *135*, 18682-18688.
- (63) Newberry, R. W.; Orke, S. J.; Raines, R. T., *Org. Lett.* **2016**, *18*, 3614-3617.
- (64) Bartlett, G. J.; Choudhary, A.; Raines, R. T.; Woolfson, D. N., *Nat Chem Biol* **2010**, *6*, 615-620.
- (65) Newberry, R. W.; VanVeller, B.; Guzei, I. A.; Raines, R. T., *J. Am. Chem. Soc.* **2013**, *135*, 7843-7846.
- (66) Choudhary, A.; Gandla, D.; Krow, G. R.; Raines, R. T., *J. Am. Chem. Soc.* **2009**, *131*, 7244-7246.
- (67) Fischer, F. R.; Wood, P. A.; Allen, F. H.; Diederich, F., *Proc. Natl. Acad. Sci.* **2008**, *105*, 17290-17294.
- (68) Dominelli-Whiteley, N.; Brown, J. J.; Muchowska, K. B.; Mati, I. K.; Adam, C.; Hubbard, T. A.; Elmi, A.; Brown, A. J.; Bell, I. A. W.; Cockroft, S. L., *Angew. Chem. Int. Ed.* **2017**, *56*, 7658-7662.
- (69) In addition, NBO calculations revealed no such secondary interactions.
- (70) Yang, L.; Adam, C.; Nichol, G. S.; Cockroft, S. L., *Nat. Chem.* **2013**, *5*, 1006-1010.
- (71) Sarwar, M. G.; Dragisic, B.; Salsberg, L. J.; Gouliaras, C.; Taylor, M. S., *J. Am. Chem. Soc.* **2010**, *132*, 1646-1653.
- (72) Robertson, C. C.; Perutz, R. N.; Brammer, L.; Hunter, C. A., *Chem. Sci.* **2014**, *5*, 4179-4183.
- (73) Yang, L.; Brazier, J. B.; Hubbard, T. A.; Rogers, D. M.; Cockroft, S. L., *Angew. Chem. Int. Ed.* **2016**, *55*, 912-916.
- (74) Stone, A. J.; Price, S. L., *J. Phys. Chem.* **1988**, *92*, 3325-3335.
- (75) Bent, H. A., *Chem. Rev.* **1968**, *68*, 587-648.
- (76) Reed, A. E.; Curtiss, L. A.; Weinhold, F., *Chem. Rev.* **1988**, *88*, 899-926.
- (77) Gonthier, J. F.; Steinmann, S. N.; Wodrich, M. D.; Corminboeuf, C., *Chem. Soc. Rev.* **2012**, *41*, 4671-4687.
- (78) Grabowski, S. J., *Chem. Rev.* **2011**, *111*, 2597-2625.
- (79) Alabugin, I. V.; Zeidan, T. A., *J. Am. Chem. Soc.* **2002**, *124*, 3175-3185.
- (80) Weinhold, F.; Landis, C. R., *Chem. Ed. Res. Pract.* **2001**, *2*, 91-104.
- (81) Our findings rule out a purely electrostatic model for chalcogen-bonding interactions, though they may be, at least qualitatively, compatible with an electrostatic plus polarization model. Murray, J. S.; Politzer, P., *Wiley Interdiscipl. Rev. Comp. Mol. Sci.* **2017**, DOI: 10.1002/wcms.1326.

